Published in: Journal of Physics and Chemistry of Solids (2011), vol. 72, pp. 158-163.
Status: Postprint (Author's version)

Spray drying: An alternative synthesis method for polycationic oxide compounds

B. Rivas-Murias[a], J.-F. Fagnard[b], Ph. Vanderbemden[b], M. Traianidis[c], C. Henrist[a], R. Cloots[a], B. Vertruyen[a]

[a] *SUPRATECS/Inorganic Materials Chemistry, B6, University of Liège, B-4000 Liège, Belgium*

[b] *SUPRATECS/Electrical Measurements and Instrumentation, B28, University of Liège, B-4000 Liège, Belgium*

[c] *Belgian Ceramic Research Centre, Mons, Belgium*

ABSTRACT

Synthesis of polycationic compounds by the spray-drying technique is an interesting alternative in the domain of aqueous precursor synthesis methods. Spray drying yields high quality samples with good reproducibility. The possibility of scaling up for production of large quantities with fast processing time is well established by the commercial availability of powders of various compositions. In this paper, we have discussed the advantages and limitations of this method and demonstrated its interest by synthesizing a few polycationic compounds selected for their attractive properties of thermoelectricity [$Bi_{1.68}Ca_2Co_{1.69}O_8$, $La_{0.95}A_{0.05}CoO_3$ (A=Ca, Sr, Ba)] or magnetoresistance [$La_{0.70}A_{0.30}MnO_3$ (A=Sr, Ba)]. We have confirmed the quality of these samples by reporting their structure, magnetic and transport properties.

Keywords : A. Oxides ; B. Chemical synthesis ; C. X-ray diffraction ; D. Electrical properties ; D. Magnetic properties

1. Introduction

Nowadays, dealing with polycationic oxides is a part of many solid-state scientists' daily routine and cationic substitution is a standard optimization tool for functional compounds. However, a homogeneous distribution of three or more cations in a polycationic oxide material may be difficult to achieve by standard solid-state synthesis. This is one of the reasons for the development of precursor synthesis methods [1], other reasons being the possibility to lower the temperature of the heat treatment and/or to obtain powders with various grain sizes. In a typical precursor synthesis, soluble salts of the cations are first dissolved in a solvent, and then a solid precursor is obtained by a process such as precipitation, sol-gel or solvent vaporization. The experimental parameters must be optimized so that the homogeneous cationic distribution in the solution is retained in the solid precursor.

Among the precursor laboratory techniques, the spray-drying method is less commonly used than sol-gel or coprecipitation but presents significant advantages such as good reproducibility and possibility of production of large quantities (see 'Discussion'). In fact, the spray-drying technique is best known as a versatile industrial process, during which a water-based suspension is transformed into a dry agglomerated powder by atomization of the suspension into a stream of hot air. This method of granulation of suspensions is frequently encountered in pharmaceutical and food industries [2]. It is also used in the field of ceramics, for the production of agglomerated granules with spherical morphologies and good flowability characteristics [3, 4]. However, this technique may also be applied to solutions [5]: the solution containing the desired cations (feedstock solution) is atomized into small droplets and injected in a hot drying chamber. Solvent vaporization occurs and the resulting solid particles are separated from the air flow in the cyclone and collected in a container.

Recently, spray drying of solutions has been used to synthesize some polycationic oxides investigated in view of applications as magnetoresistive materials [6], high temperature superconductors [5], thermoelectric materials [7], piezoelectric materials [8] and electrode materials for lithium-ion batteries [9-11] or solid-oxide fuel cells [12]. We have recently reported another, more restricted, application, which is the preparation of composites by spontaneous phase separation of the components during the heat treatment [13].

In the present study, we have selected a few thermoelectric or magnetoresistive polycationic oxides whose synthesis by spray drying has not yet been reported in the literature. We describe the synthesis and characterization of these compounds and use them as examples for a general discussion about the advantages and limitations of the spray-drying method. The main characteristics of the selected compounds are summarized in Table 1. The structural and morphological characterization at different stages of the synthesis is reported in Section 3.1. The relevant transport and/ or magnetic properties are presented in Section 3.2, where our results are compared to data reported for samples prepared by other techniques. Finally, in Section 4, we compare spray drying with other techniques and discuss the possible modifications of the experimental parameters if production of large quantities is considered.

Table 1 *Main characteristics of selected compounds to be synthesized by spray-drying.*

Compound name	Composition	Structure	Property
Bismuth cobaltite	$Bi_{1.68}Ca_2Co_{1.69}O_8$	Layered	Thermoelectricity
Cobalt perovskite	$La_{0.95}A_{0.05}CoO_3$ (A=Ca, Sr, Ba)	Perovskite	Thermoelectricity
Manganese perovskite	$La_{0.70}A_{0.30}MnO_3$ (A=Sr, Ba)	Perovskite	Magnetoresistance

2. Experimental

$Bi_{1.68}Ca_2Co_{1.69}O_8$, $La_{0.95}A_{0.05}CoO_3$ (A=Ca, Sr, Ba) and $La_{0.70}A_{0.30}MnO_3$ (A=Sr, Ba) samples were synthesized by heat treatment of precursor powders obtained by the spray-drying method.

Aqueous acetic acid feedstock solutions were prepared from stoichiometric amounts of acetates (for lanthanum, bismuth, manganese and cobalt) and carbonates (for calcium, strontium and barium). The exact stoichiometry of the reagents was ascertained by chemical titration or thermogravimetric analysis. The total cation concentration of the feedstock solution was ~0.1 mol/l for the bismuth cobaltite and ~0.3-0.4 mol/l for the cobalt and manganese perovskites. The solution pH was ~5.

Spray drying was performed in a lab-scale apparatus Büchi B-191 through a co-current atomizer (i.e., sprayed solution and drying air flow in the same direction) using a 0.7 mm nozzle. The inlet temperature was 200 °C with a liquid feed rate of 1.4 ml/min. The process was carried out in air, using a flow rate of 700 normal l/h. The outlet temperature during spraying was 145-150 °C.

After spray drying, the precursor powders were calcined at 600 °C for 2 h in air, with a slow heating rate (25 °C/h). These powders were then further heated in air at different temperatures (see 'Results' section). Depending on composition, maximum temperature never exceeded 850 °C (for 10 h) in the case of the bismuth cobaltite and 1300 °C (for 40 h) in the case of the perovskites. In all cases, the powders were uniaxially pressed into 13 mm diameter pellets before the last step of the heat treatment.

Powder X-ray diffraction (XRD) was performed using a Siemens D5000 diffractometer with Cu(K_α) radiation, in the 2θ range from 20° to 62° with a step size of 0.030°. Thermogravimetric Analysis (TGA) and Differential Scanning Calorimetry (DSC) were carried out using a Netzsch STA449C apparatus. The morphology and size of the particles were studied by scanning electron microscopy (Philips XL30 FEG-ESEM) and the cationic composition was checked by energy-dispersive X-ray analysis (EDAX). In addition, some of the samples were analyzed by inductively coupled plasma optical emission spectroscopy (ICP-OES, Perkin Elmer Optima 4300 DV). The density of the pellets was measured by Archimedes' method in 1-butanol.

The magnetic response was measured as a function of magnetic field with a Vibrating Sample Magnetometer (VSM) from Oxford Instruments. The dc magnetic moment (zero-field-cooled and field-cooled, 50 mT) and the electrical resistivity were measured at 20-400 K using a Quantum Design Physical Property Measurement System. The electrical conductivity and thermoelectric power were measured by a RZ2001i device (Ozawa Science) at 300-1250 K.

Published in: Journal of Physics and Chemistry of Solids (2011), vol. 72, pp. 158-163.
Status: Postprint (Author's version)

3. Results

3.1. Structural and microstructural characterization

All as-sprayed powders were found to be amorphous by X-ray diffraction (XRD). Thermal analysis in air was used to investigate the thermal decomposition of the precursors and to choose the subsequent heat treatment. Data for the bismuth cobaltite precursor are shown in Fig. 1. Qualitatively similar results were obtained for the other compounds. Residual water departs in the lower temperature range, due to water desorption and hydrate decomposition. The major weight loss, together with a sharp exothermic peak, occurs in the 250-300 °C range, as also found for the acetate reagents. This is followed by a progressive weight loss, typically up to 630-650 °C.

Fig. 1. *Thermal analysis of the spray-dried precursor of bismuth cobaltite: weight loss (solid line) and differential scanning calorimetry signal (dashed line).*

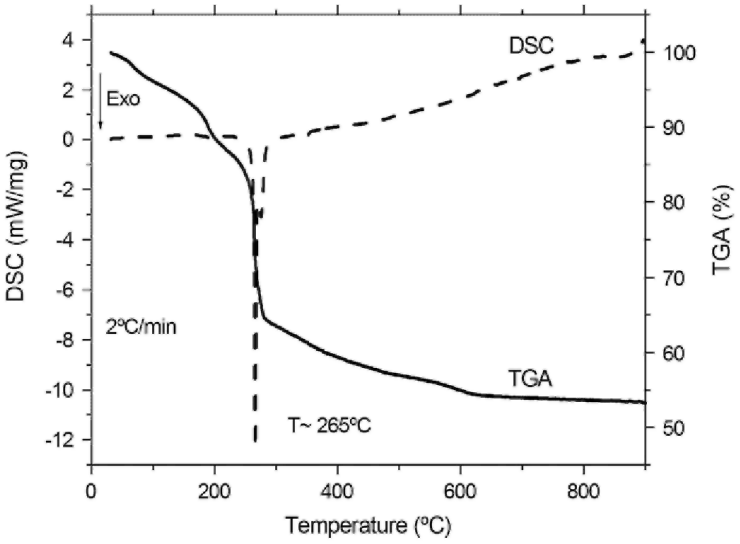

Fig. 2. *X-ray diffraction pattern for the $La_{0.70}Sr_{0.30}MnO_3$ sample at different synthesis temperatures: (a) 900°C/10h and (b) 1300°C/40h. The small peak at ~29.1° corresponds to the K_β (1 0 4) reflexion (R-3c space group). Inset: Zoom between 32° and 33.2°.*

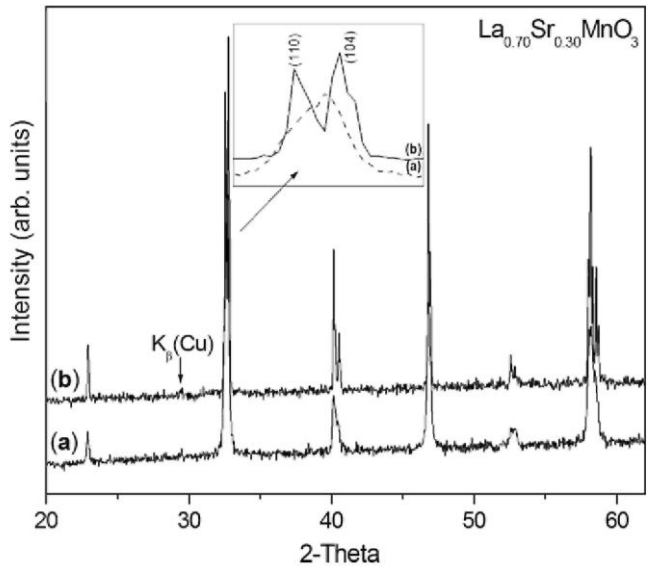

The progress of the crystallization was studied by collecting XRD patterns of samples heated at different temperatures. For all compositions, the reflections of the desired phase were already present after a treatment at 600 °C (2 h) but the peaks are broad and intermediate phases (such as $La_2O_2CO_3$ or β-Bi_2O_3) were detected. After 10 h at 850 °C (bismuth cobaltite) or at 900 °C (perovskites), single-phase patterns were obtained. However, in the case of the perovskites, the peaks were still broad and the crystallinity could be improved by heating to higher temperatures. As an example, Fig. 2 compares the XRD pattern of the $La_{0.70}Sr_{0.30}MnO_3$ sample treated at 900 °C with that at 1300 °C: in the case of the sample treated at 1300 °C, the peaks are much narrower, so that the (1 1 0) and (1 0 4) reflections are resolved (inset Fig. 2).

For all compounds, the cell parameters were refined from the XRD patterns of the best-crystallized samples (i.e., bismuth cobaltite treated at 850 °C and perovskites treated at 1300 °C). The bismuth cobaltite crystallizes in an incommensurate layered structure, with two monoclinic subsystems alternating along the c axis: a CoO_2 layer formed by edge sharing CoO_6 octahedra and a rock salt (RS)-type block [14]. The full pattern matching analysis was performed using the Jana2000 software [15]. The cell parameters are a = 4.89(6) Å, b_1 = 4.72(2) Å, b_2 = 2.78(7) Å, c = 14.70(2) Å and β = 93.5(9)°, where b_1 and b_2 are the b parameters for the RS block and the CoO_2 layer, respectively. These values are close to those reported in the literature [16]. The XRD patterns of all perovskite samples could be refined in the R3c space group with the Rietica software [17]. The lattice parameters and cell volume are listed in Table 2 and are in good agreement with the data reported in literature for these compounds [18-23].

Fig. 3. *Scanning electron micrographs of the bismuth cobaltite at different stages of synthesis: (a) spray-dried precursor, (b) after heat treatment at 600 °C and (c) after heat treatment at 850 °C.*

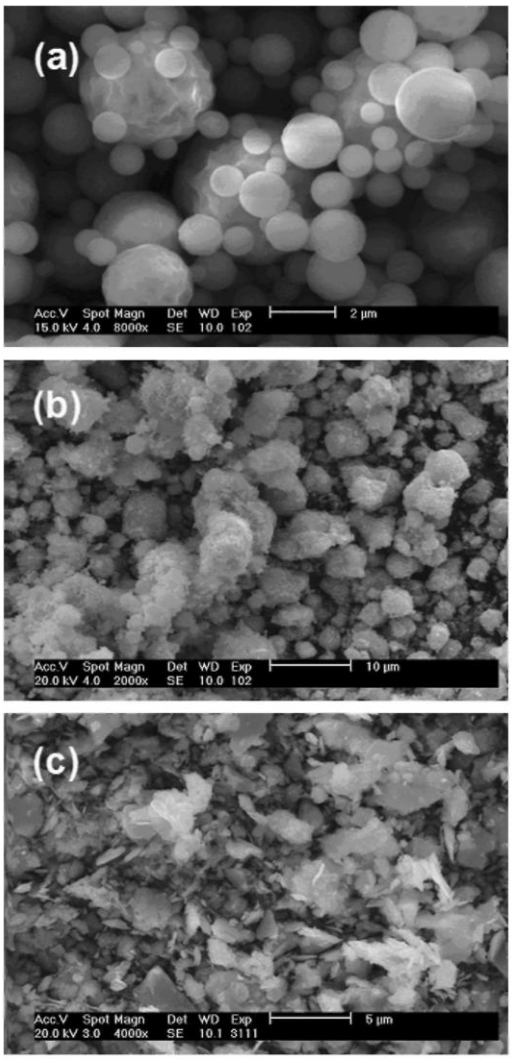

Table 2 *Cell parameters and cell volume (R3c space group) of the perovskite samples sintered at 1300 °C.*

	$La_{0.95}Ca_{0.05}CoO_3$	$La_{0.95}Sr_{0.05}CoO_3$	$La_{0.95}Ba_{0.05}CoO_3$	$La_{0.70}Sr_{0.30}MnO_3$	$La_{0.70}Ba_{0.30}MnO_3$
a (Å)	5.4392 (2)	5.4436 (3)	5.4491 (3)	5.5040 (3)	5.5373 (3)
c (Å)	13.0885 (3)	13.1117 (6)	13.1416 (6)	13.3553 (8)	13.4979 (6)
V (Å^3)	335.34 (2)	336.48 (3)	337.93 (6)	350.39 (4)	358.42 (3)

The microstructure of all compounds at the different stages of the synthesis was characterized by scanning electron microscopy, as illustrated in Fig. 3, for the bismuth cobaltite. As-sprayed particles (Fig. 3a) display a typical spherical shape. Irregular particles of a few microns are obtained after the treatment at 600 °C (Fig. 3b) and transform into platelets (Fig. 3c) after treatment at 850 °C, due to the layered structure of bismuth cobaltite. The perovskite structure has no such anisotropy; therefore the particles (not shown here) do not display any aspect ratio peculiarities.

Polished cross-sections of pellets of all compositions were also characterized in the scanning electron microscope: back scattering electron imaging and energy-dispersive X-ray analysis confirmed the chemical homogeneity and the good agreement with the nominal compositions. In addition, ICP-OES analyses were carried out for three selected samples. The results ($La_{0.73\pm0.03}Sr_{0.30\pm0.01}Mn_{1\pm0.02}O_3$, $La_{0.90\pm0.03}Sr_{0.04\pm0.01}Co_{1\pm0.01}O_3$ and $Bi_{1.60\pm0.05}Ca_{2\pm0.01}Co_{1.82\pm0.02}O_8$) are in agreement with the EDAX data except for a 7% Co excess in the bismuth cobaltite sample. The density of these pellets was measured by Archimedes' method. Porosity was ~25% for bismuth cobaltite and between 3% and 6% for the manganese and cobalt perovskites, respectively.

3.2. Magnetic, transport and/or thermoelectrical properties

Measuring the physical properties is an efficient way to confirm the quality of the samples by comparison with literature data. In the following, relevant properties are measured on the spray-dried samples sintered at 850 °C (bismuth cobaltite) or 1300 °C (perovskites), i.e., a standard high temperature treatment because the objective is to favor a good homogeneity of the cationic distribution. Readers interested in a systematic investigation of the influence of the heat treatment on the properties of spray-dried samples are referred to our previous work [6] on a related compound ($La_{0.7}Ca_{0.3}MnO_3$), sintered at temperatures varying from 800 to 1250 °C.

Both the bismuth cobaltite and the cobalt perovskites are known to display thermoelectrical properties [24-28]. In Fig. 4, the electrical conductivity (σ) and the Seebeck coefficient (S) are plotted in the temperature range of 300-1250 K. In the case of bismuth cobaltite (Fig. 4a), σ decreases when the temperature increases. On the other hand, the Seebeck coefficient increases almost linearly. As a result, the power factor PF = $S^2\sigma$ reaches a maximum value of 1.6 μW K^{-2} cm^{-1} at ~1050 K. The Seebeck results are in good agreement with those reported for a solid-state sample at room temperature [24] and the value of the power factor is comparable to the value obtained by hot-forging method [25]. For the cobalt perovskites (Fig. 4b), the electrical conductivity increases with temperature up to 700 K and then decreases slightly. The obtained values are slightly higher than those reported in the literature [18,28,29]. The Seebeck coefficient (Fig. 4b) decreases when the temperature increases up to ~600 K and then tends to a constant value above 800 K. This behavior agrees well with that reported in the literature [18,28,30]. In the investigated temperature range, the highest power factor values PF = $S^2\sigma$ are obtained at room temperature: 4 μW K^{-2} cm^{-1} for $La_{0.95}Sr_{0.05}CoO_3$ and $La_{0.95}Ba_{0.05}CoO_3$ and 3.4 μW K^{-2} cm^{-1} for $La_{0.95}Ca_{0.05}CoO_3$. These values are somewhat higher than the power factor reported in Ref. [28] for $La_{0.95}Sr_{0.05}CoO_3$ but are much smaller than the value reported by Androulakis et al. [27], who found an unusually large Seebeck coefficient (700 μV K^{-1} at 300 K).

The cobalt perovskites were also characterized by low-temperature magnetic measurements since the irreversibility temperature is a parameter that can be compared to literature data (see 'Discussion'). The temperature dependence of the zero-field-cooled (ZFC) and field-cooled (FC) susceptibilities for $La_{0.95}Sr_{0.05}CoO_3$ is shown in Fig. 5. The ZFC and FC curves merge at some temperature T_{cusp}~18 K. The $La_{0.95}Ca_{0.05}CoO_3$ and $La_{0.95}Ba_{0.05}CoO_3$ data are qualitatively similar to $La_{0.95}Sr_{0.05}CoO_3$, with T_{cusp}~18 and 20 K for the Ca- and Ba-substituted samples, respectively.

Published in: Journal of Physics and Chemistry of Solids (2011), vol. 72, pp. 158-163.
Status: Postprint (Author's version)

Fig. 4. *Seebeck coefficient (left axes, full symbols) and electrical conductivity (right axes, open symbols) for (a) $Bi_{1.68}Ca_2Co_{1.69}O_8$ and (b) $La_{0.95}A_{0.05}CoO_3$.*

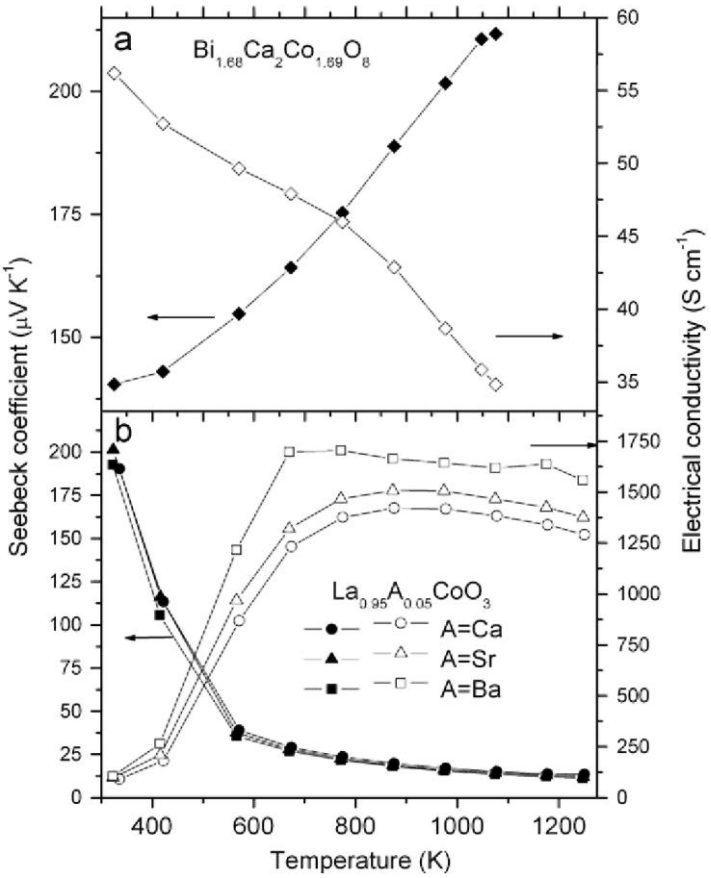

Fig. 5. *ZFC and FC magnetic susceptibility curves for $La_{0.95}Sr_{0.05}CoO_3$ sintered at 1300 °C.*

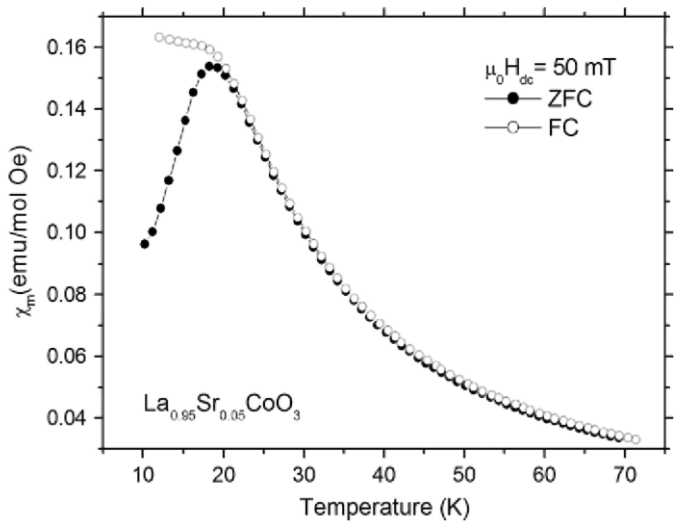

Fig. 6. *Electrical resistivity without (full symbols) and with (open symbols) external magnetic field and magnetoresistance response for $La_{0.70}Sr_{0.30}MnO_3$ and $La_{0.70}Ba_{0.30}MnO_3$ (solid lines) samples sintered at 1300 °C.*

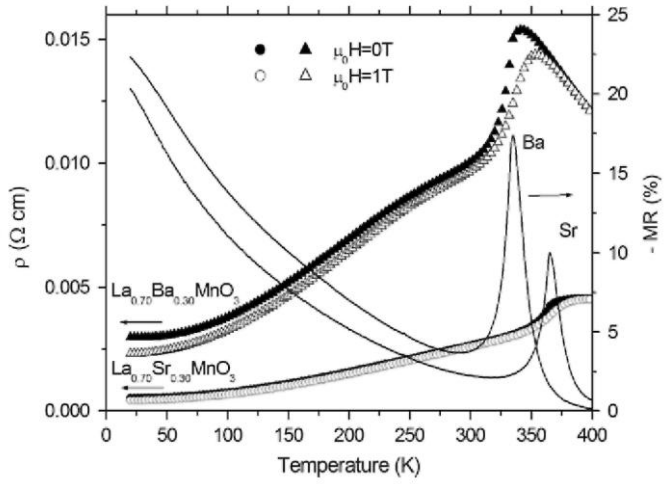

The manganese perovskites studied here are known for their colossal magnetoresistance properties [31-33]. Fig. 6 shows the temperature dependence of the resistivity in zero magnetic field (ρ_0) and the resistivity in 1 T magnetic field (ρ_H). The corresponding magnetoresistance MR(%) = [(ρ_H-ρ_0)/ρ_0]100 is also shown in Fig. 6. The $La_{0.70}Sr_{0.30}MnO_3$ sample exhibits a resistive transition between two metallic-like states at 364 K, while the resistive transition in $La_{0.70}Ba_{0.30}MnO_3$ occurs at 334 K from a metallic-like state at $T < T_C$ (where T_C is the Curie temperature) to an insulating state at $T > T_C$. These transition temperatures are in good agreement with the data reported in the literature [19,34,35]. The magnetoresistance curves display a peak in the vicinity of the resistive transition, while the maximum magnetoresistance (about - 20% under 1 T) is observed at low temperature. Resistivity vs. magnetic field cycles at 20 and 77 K (not shown) display the usual low-field and high-field effects. Magnetization vs. magnetic field measurements confirm that both $La_{0.70}Sr_{0.30}MnO_3$ and $La_{0.70}Ba_{0.30}MnO_3$ are ferromagnetic below the transition temperature: the saturation magnetizations at 20 K are ~3.8μ_B/Mn for $La_{0.70}Sr_{0.30}MnO_3$ and ~3.6μ_B/Mn for $La_{0.70}Ba_{0.30}MnO_3$, which are in good agreement with the calculated spin-only values and with the experimental data reported in literature [34].

4. Discussion

The good agreement of our experimental results (Section 3.2) with literature data confirms that the spray-drying method can be used to prepare high quality samples with satisfactory cationic distribution. In this respect, the case of the $La_{0.95}Sr_{0.05}CoO_3$ sample is worth a comment. The results of magnetic susceptibility (see Fig. 5) obtained here forthe spray-dried sample (T_{cusp}~20 K) agree well with the behavior reported by Nam et al. [36], whereas other authors [29,37,38] found an irreversibility temperature of ~200 K. The main difference between these literature reports is the duration of the heat treatment: the sample of Nam et al. [36] was prepared by solid-state reaction using a 2-month heat treatment. These authors stressed the importance of a homogeneous distribution of strontium cations to prevent any ferromagnetic cluster effects [36]. Indeed in the $La_{1-x}Sr_xCoO_3$ and $La_{1-x}Ba_xCoO_3$ systems with x below ~0.20, the magnetic behavior is known to be dominated by a frustration state (spin-glass phase), due to the opposition between antiferromagnetic superexchange (Co^{3+}-Co^{3+} and Co^{4+}-Co^{4+} interactions) and ferromagnetic double exchange (Co^{3+}-Co^{4+} interactions) [30,37-39]. In the present work, our sample prepared from a spray-dried precursor displays properties similar to the sample of Nam et al. [36] but with a much shorter heat treatment (40 h).

Since spray drying appears as a valuable synthesis method for polycationic oxides, the following section is devoted to the discussion on its advantages and limitations. We will restrict ourselves to the case of spray drying of aqueous solutions, since most systems are not designed for organic solvents and aqueous solutions are preferable in any case. It must also be noted that the spray dryer used in this work is a lab-scale system, optimized for synthesis in small quantities (typically a few grams) and ease of cleaning. However, this device presents disadvantages by comparison with large-scale equipments, such as limited drying power (thus slow feedstock solution flow) and poor yield (~60-70%, mainly due to powder sticking to walls of the drying chamber). Therefore, we also discuss the possible modifications of experimental conditions in the case of production in large quantities.

The concentration of the feedstock solution is an important parameter of the spray-drying process. The quantity of solvent to evaporate is smaller if high concentrations are used. This means that, taking into account the maximum "drying performance" of each spray dryer, increase in the concentration allows us to increase the solution flow rate, and thereby decrease the time needed to prepare a given quantity of material. It should be noted that the concentration of the solution also affects the size of the as-sprayed powder [6]: higher concentration of the solution usually results in larger particles. The maximum concentration is controlled by the solubility of the salts in water. This limits the use of spray drying to compounds for which water-soluble salts can be found. Commercial nitrates or acetates are especially useful in research work, when a number of different compositions are prepared. Nitrates are often chosen due to their usual high solubility. However, some nitrates are so hygroscopic that the sprayed powder can re-adsorb water before being collected. This is why acetates were used in the present work. Nevertheless, these salts are more expensive than the oxides and their exact stoichiometry should be checked before use. If a specific composition is chosen for production in larger amounts, it is cheaper to prepare stock solutions by dissolution of the appropriate oxides or carbonates in nitric and/or acetic acid (adjustment of the solution pH may be necessary).

In fact, the choice of the anion (nitrate, acetate, among others) affects not only the maximum possible concentration of the feedstock solution but also the intermediate phases in the subsequent heat treatment steps. The decomposition pathway during the heat treatment influences the possible formation of small amounts of poorly crystallized intermediate phases. For example, $La_2O_2CO_3$ formation is frequently reported in low-temperature synthesis of lanthanum compounds using carbonaceous precursors [6,40]. This is the case in this work, as reported in Section 3.1. Nitrates would probably be better in that respect but are too hygroscopic to be used in our lab-scale system, as explained above. A possible modification in the set-up would be to insert a tubular furnace at the exit of the drying chamber to enhance the drying of the precursor. In the case of oxide synthesis, partial decomposition of the salts at that stage would not be a problem since these precursors have to be calcined after spray drying.

This necessity of a subsequent heat treatment means that spray-drying synthesis of oxides is not a "very-low-temperature" method such as, for example, hydrothermal synthesis in autogenous pressure or precipitation in highly basic solution [41], which may yield highly crystallized particles at temperatures below 250 °C but are restricted to a rather limited number of compounds. The spray-drying method described here is a competitor of other precursor laboratory techniques such as sol-gel, coprecipitation or combustion. One of the main advantages of spray drying is the possibility to increase the quantity of prepared material without modifying the characteristics of the resultant precursor powder. In the case of spray drying, this is easily done just by spraying a larger volume. On the contrary, techniques such as sol-gel or combustion usually involve an exothermic decomposition step: increasing the quantities often leads to higher local temperature due to heat conduction issues. Coprecipitation syntheses do not suffer from such problems but may be quite lengthy to optimize in the case of polycationic compounds, due to the different solubilities of the cations. Differential precipitation is not such an issue in spray drying because precipitation (due to solvent evaporation) occurs at the scale of the solution droplet in the drying chamber of the system. Another major advantage of spray drying is its reproducibility, which we were able to appreciate when preparing several batches of a given compound.

In summary, spray drying is an easy synthesis method, scalable and reproducible. It can be used to obtain single-phase materials at temperature lower than the usual solid-state method. The technique can also be combined with a standard high temperature treatment: in this case, the objective is to favor a good homogeneity of the cationic distribution. This was the approach selected for the samples whose physical properties are presented in Section 3.2. A systematic investigation of the influence of the heat treatment on the properties of spray-dried samples can be found in our previous work [6] on $La_{0.7}Ca_{0.3}MnO_3$ samples sintered at temperatures varying from 800 to 1250 °C.

5. Conclusion

A few representative polycationic compounds were selected to illustrate the interest of the spray-drying method forthe preparation of functional oxide materials. $Bi_{1.68}Ca_2Co_{1.69}O_8$, $La_{0.95}A_{0.05}CoO_3$ (A=Ca, Sr, Ba) and $La_{0.70}A_{0.30}MnO_3$ (A=Sr, Ba) samples were synthesized by spray drying followed by a heat treatment. The high quality of the samples was confirmed by measuring the electrical, magnetic and thermoelectric properties and the results obtained were in good agreement with those reported in the literature.

Our results confirm that spray drying is an interesting alternative synthesis method for many polycationic oxides. Major advantages in comparison with other precursor synthesis methods are the good reproducibility and the possibility of scaling up, by going from a lab-scale equipment to a (semi)-industrial system for production of

large quantities with fast processing time. Even in the framework of academic studies, it may be attractive to produce somewhat larger quantities of powders by spraying a larger volume in a lab-scale system, for example for characterization methods such as neutron diffraction experiments or sintering optimization.

Acknowledgments

Part of this work was supported by the Belgian Science Policy under the Technology Attraction Pole Program (CHEMAT TAP2/03). The authors thank H. Muguerra for his help with the X-ray refinement using the Jana2000 software. We also thank the ICP-OES service of the C.A.C.T.I (University of Vigo) for the ICP analyses.

References

[1] D. Segal, J. Mater. Chem. 7 (1997) 1297-1305.

[2] M.-I. Re, Dry. Technol. 16 (1998) 1195-1236.

[3] S.J. Lukasiewicz, J. Am. Ceram. Soc. 72 (1989) 617-624.

[4] A. Schrijnemakers, S. Andre, G. Lumay, N. Vandewalle, F. Boschini, R. Cloots, B. Vertruyen, J. Eur. Ceram. Soc. 29 (2009) 2169-2175.

[5] D. Depla, R. Mouton, S. Hoste, J. Eur. Ceram. Soc. 17 (1997) 153-159.

[6] B. Vertruyen, A. Rulmont, R. Cloots, J.-F. Fagnard, M. Ausloos, I. Vandriessche, S. Hoste, J. Mater. Sci. 40 (2005) 117-122.

[7] T. Motohashi, Y. Nonaka, K. Sakai, J. Appl. Phys. 103 (2008) 033705.

[8] F. Bezzi, A.L. Costa, D. Piazza, A. Ruffini, S. Albonetti, C. Galassi, J. Eur. Ceram. Soc. 25 (2005) 3323-3334.

[9] F. Gao, Z. Tang, J. Xue, Electrochim. Acta 53 (2007) 1939-1944.

[10] A. Ito, D. Li, Y. Lee, K. Kobayakawa, Y. Sato, J. Power Sources 185 (2008) 1429-1433.

[11] H.M. Wu, J.P. Tu, X.T. Chen, Y.F. Yuan, Y. Li, X.B. Zhao, G.S. Cao, J. Power Sources 159 (2006) 291-294.

[12] S. Bebelis, N. Kotsionopoulos, A. Mai, F. Tietz, J. Appl. Electrochem. 37 (2007) 15-20.

[13] B. Vertruyen, R. Cloots, M. Ausloos, J.-F. Fagnard, Ph. Vanderbemden, Phys. Rev. B 75 (2007) 165112.

[14] H. Leligny, D. Grebille, O. Pérez, A.C. Masset, M. Hervieu, C. Michel, B. Raveau, Acta Cryst. B 56 (2000) 173-182.

[15] V. Petricek, M. Dusek, L Palatinus, Jana 2000: Crystallographic Computing System, Institute of Physics, Prague, 2000.

[16] H. Muguerra, D. Grebille, E. Guilmeau, R. Cloots, Inorg Chem. 47 (2008) 2464-2471.

[17] C.J. Howard, B.A. Hunter, Rietica: "A computer program for Rietveld analysis of X-ray and neutron powder diffraction patterns", Australian Nuclear Science and Technology Organization, Lucas Heights Research Laboratories.

[18] A.J. Zhou, T.J. Zhu, X.B. Zhao, J. Mater. Sci. 43 (2008) 1520-1524.

[19] H.L. Ju, Y.S. Nam, J.E. Lee, H.S. Shin, J. Magn. Magn. Mater. 219 (2000) 1-8.

[20] V.A. Cherepanov, L.Ya. Gavrilova, E.A. Filonova, M.V. Trifonova, V.I. Voronin, Mater. Res. Bull. 34 (1999) 983-988.

[21] P.G. Radaelli, G. Iannone, M. Marezio, H.Y. Hwang, S.-W. Cheong, J.D.Jorgensen, D.N. Argyriou, Phys. Rev. B 56 (1997) 8265-8276.

[22] Z. El-Fadli, M.R. Metni, F. Sapina, E. Martinez, J.-V. Folgado, A. Beltran, Chem. Mater. 14 (2002) 688-698.

[23] I.G. Krogh Andersen, E. Krogh Andersen, P. Norby, E. Skou, J. Solid State Chem. 113 (1994) 320-326.

[24] A. Maignan, S. Hébert, M. Hervieu, C. Michel, D. Pelloquin, D. Khomskii, J. Phys.: Condens. Matter 15 (2003) 2711-2723.

[25] E. Guilmeau, M. Mikami, R. Funahashi, J. Mater. Res. 20 (2005) 1002-1008.

[26] R. Funahashi, I. Matsubara, S. Sodeoka, Appl. Phys. Lett. 76 (2000) 2385-2387.

[27] J.Androulakis, P. Migiakis, J.Giapintzakis, Appl. Phys. Lett. 84 (2004) 1099-1101.

[28] K. Iwasaki, T. Ito, T. Nagasaki, Y. Arita, M. Yoshino, T. Matsui, J. Solid State Chem 181 (2008) 3145-3150.

[29] P. Mandal, P. Choudhury, S.K. Biswas, B. Ghosh, Phys. Rev. B 70 (2004) 104407.

[30] S.R. Sehlin, H.U. Anderson, D.M. Sparlin, Phys. Rev. B 52 (1995) 11681-11689.

[31] R. von Helmolt, J. Wecker, B. Holzapfel, L. Schultz, K. Samwer, Phys. Rev. Lett. 71 (1993)2331-2333.

[32] S.Jin, T.H. Tiefel, M. McCormack, R.A. Fastnacht, R. Ramesh, L.-H. Chen, Science 264(1994)413-415.

[33] K. Chahara, T. Ohno, M. Kasai, Y. Kozono, Appl. Phys. Lett. 63 (1993) 1990-1992.

[34] S.V. Trukhanov, J. Mater. Chem. 13 (2003) 347-352.

[35] A. Urushibara, Y. Moritomo, T. Arima, A. Asamitsu, G. Kido, Y. Tokura, Phys. Rev. B 51 (1995) 14103-14109.

[36] D.N.H. Nam, R. Mathieu, P. Nordblad, N.V. Khiem, N.X. Phuc, Phys. Rev. B 62 (2000) 8989-8995.

[37] C. He, M.A. Torija, J. Wu, J.W. Lynn, H. Zheng, J.F. Mitchell, C. Leighton, Phys. Rev. B 76 (2007) 014401.

[38] J. Wu, C. Leighton, Phys. Rev. B 67 (2003) 174408.

[39] M. Kriener, C. Zobel, A. Reichl, J. Baier, M. Cwik, K. Berggold, H. Kierspel, O. Zabara, A. Freimuth, T. Lorenz, Phys. Rev. B 69 (2004) 094417.

[40] A. Wold, R.J. Arnott, J. Phys. Chem. Solids 9 (1959) 176-180.

[41] F. Boschini, A. Rulmont, R. Cloots, B. Vertruyen, J. Eur. Ceram. Soc. 29 (2009) 1457-1462.